EXPERIMENTS ON SEDIMENT GRAVITY FLOWS ALONG A SLOPING FLOOR IN WATER TANKS

Honji, Hiroyuki
Research Institute for Applied Mechanics, Kyushu University : Assistant Professor

Matsunaga, Nobuhiro
Hydraulic Civil Engineering Course, Kyushu University : Postgraduate

https://doi.org/10.5109/6776443

出版情報：Reports of Research Institute for Applied Mechanics. 28 (89), pp.1-20, 1980-12. 九州大学応用力学研究所
バージョン：
権利関係：

Reports of Research Institute for Applied Mechanics
Vol. XXVIII, No. 89, 1980

EXPERIMENTS ON SEDIMENT GRAVITY FLOWS ALONG A SLOPING FLOOR IN WATER TANKS

By Hiroyuki HONJI* and Nobuhiro MATSUNAGA**

Small-scale gravity flows of glass beads, clay, salt solution, and other materials travelling down submerged sloping floors have been investigated by use of the methods of flow visualization in water tanks. Three types of gravity flows have been observed: round head type, flat front type, and internal-wave type. Behaviors and structures of these flows are demonstrated with many photographs of flow patterns.

Key words: Gravity flow, Sloping floor, Flow visualization

1. Introduction

Gravity flows take place in various situations in land and sea. Numerous investigations have been concerned with these flows, and their diverse aspects are reviewed in such recent treatises as Stanley & Swift[1], Allen[2], Komar[3], Stanley & Kelling[4], Turner[5], and Yih[6] from the geological and fluid-mechanical viewpoints.

Fluid and sediment gravity flows along subaqueous slopes are a class of gravity flows. The sediment gravity flow arising on a continental slope is referred to as 'turbidity current', and still the central subject of many marine-geological investigations (Middleton & Hampton[7]). However, laboratory studies of these types of flows by means of flow visualization are rather scarce except some recent ones, which Simpson[8] and Simpson & Britter[9] carried out on gravity flows along a horizontal floor.

This paper is concerned with visual demonstration of the behaviors and structures of diverse types of sediment and fluid gravity flows along a slope, and many photographs of their flow patterns will be included.

* Assistant Professor, Research Institute for Applied Mechanics, Kyushu University, Fukuoka 812, Japan.
** Postgraduate, Hydraulic Civil Engineering Course, Kyushu University, Fukuoka 812, Japan.

2. Experimental methods

Flow visualization experiments were carried out by using several water tanks. A typical set-up using the largest tank is shown in Fig. 1; in this glass-sided water tank filled with water a channel made of acrylic resin plates was set with a slope θ to the horizontal. The illustrated channel was 180 cm in length, 11 cm in depth and 6 cm in width, and θ could be varied from about 8 up to about 40°. A reservoir was attached to the upper end of the channel in order to keep sediment materials such as fine glass beads and pearl clay, or fluids (heavier than water) such as salt solution and glycerin-water solution.

The median diameter D of the glass beads ranged from 60 to 500 μm, and that of pearl clay was 6 μm. The density of glass beads and pearl clay was 2.4 g/cm^3. These materials in the reservoir were released by opening a gate and allowed to flow down the channel floor. A slice of the water parallel to the direction of flow was illuminated by the intense light projected through a slit as shown in Fig. 1. Flow patterns of the gravity flows were photographed by a camera, which was at rest with respect to the channel.

3. Results and discussions

Depending on various factors related to the sediment, gravity flows show diverse behaviors and structures. In this paper, the flows are distinguished roughtly into three types on the basis of their behaviors and structures as illustrated in Fig. 2. The flow of type A is a flat front gravity flow and that of type B an internal-wave type flow. The flow of type C, which consists of a round head, depressed neck and body, is the most common one, and may be called round head type.

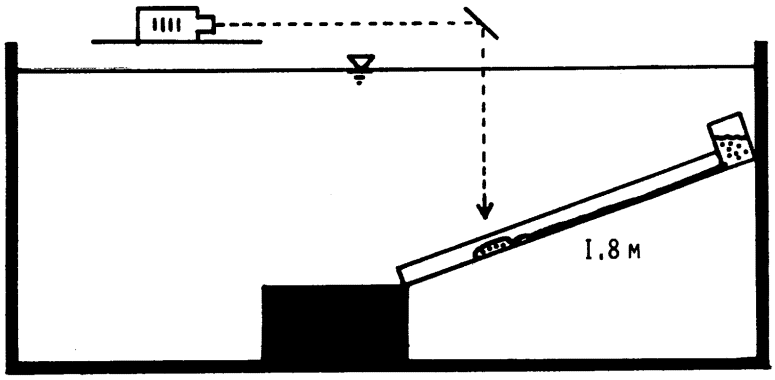

Fig. 1 Experimental set-up.

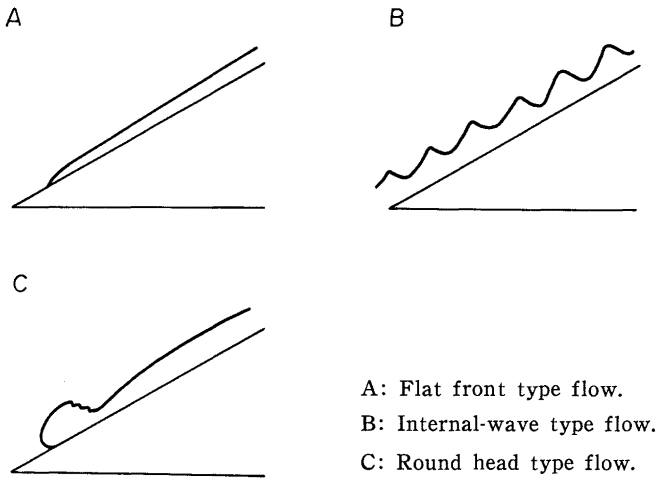

Fig. 2 Three types of gravity flows.

A gravity flow shown in Fig. 3 belongs to type A. Its front moved down a slope at a velocity of about 0.7 cm/s. Figures 4(a) to (d) show a variation of the form of type B flow; t is the time passed after Fig. 4(a) has been photographed. The body of this flow consisted of a double-layer as shown in a close-up view in Fig. 4(e). The upper sediment with the thickness of about 2.5 cm was moving upwards along the slope, and the lower with the thickness of about 1.5 cm was moving down the slope. The opposite direction of the motion is due to the effect of the so-called lock exchange. In Figs. 4(a) and (b), the upper interfaces show up a cusped wavy distortion of which the wave length was 4.9 cm. The cusped wave crest moved upwards along a slope. It was observed that upright whiskers were rising from each crest. As time went on, the interface became flat as shown in Fig. 4(c), but cusped after flattening. The cusped distortion and flattening of the uppermost interface repeated with a period of about 20 s. Figure 5 shows a travel-time curve for an upward moving crest of the flow shown in Fig. 4; time T is measured from a certain reference time. The velocity of the crest was about 0.56 cm/s.

Figures 6(a) to (c) show respectively the head, neck, and body regions of a typical type C gravity flow. The head is rounded and the neck depressed. Mixing between fresh water and sediment material is very vigorous in the body region, which shows up the so-called 'lobate structure'. Figure 7 shows a travel-time curve for the head of a type C flow after it has passed through a certain point on the sloping floor. It was moving down with a velocity of about 1.4 cm/s. This paper concerns with type C flows mainly.

Figure 8 shows the lobate structure of a gravity flow of pearl clay. A

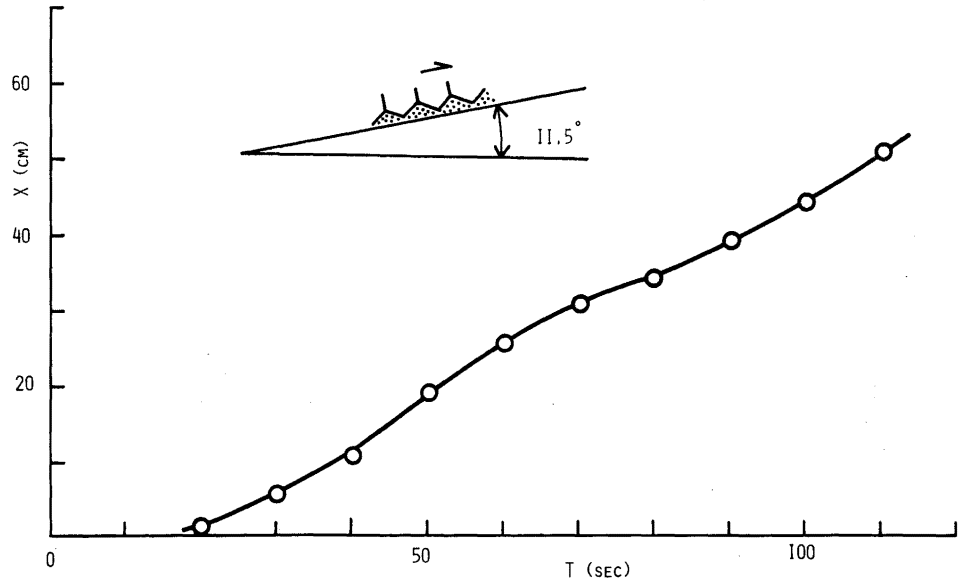

Fig. 5 Travel-time curve for a crest of type B flow;
D=130 μm, θ=11.5°.

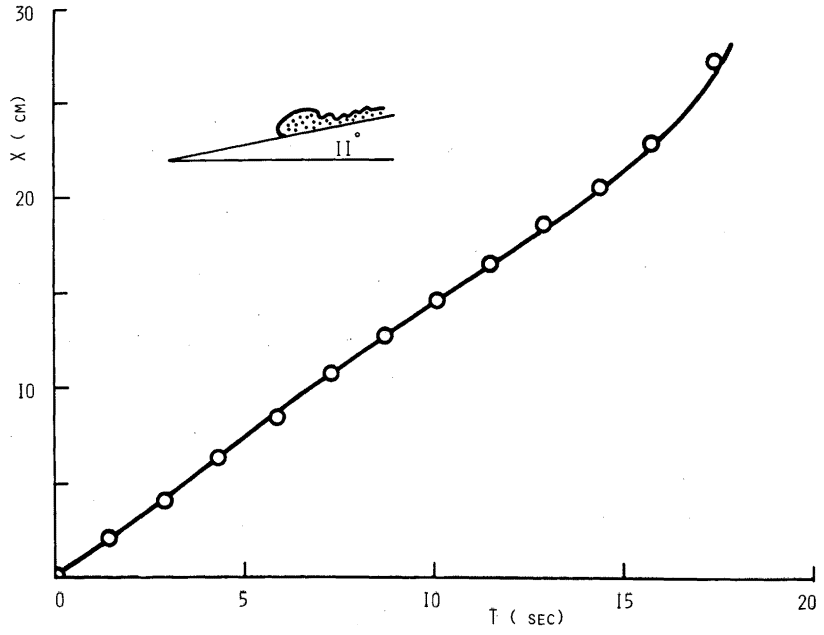

Fig. 7 Travel-time curve for the head of a type C flow;
D=47 μm, θ=11°.

similar, but more fully developed, structure is shown also in Fig. 9. The lobate structure of the body may be caused by an instability of turbulent shear flow. Figure 10 shows the velocity fluctuation in a gravity flow of a salt-solution; the height of a hot-film probe was 1.5 cm above the floor of a channel. In the figure, time is increasing from left to right; the time scale indicated is 0.68 s. The first spike shows the passage of the head. The lower spikes following it indicate that the body is passing by. After the passage of the turbulent body region, several regular spikes appear. Possibly, these spikes correspond to the passage of the lobate body.

In Figs. 11(a) to (c) are shown unsteady streamline patterns for the motion of a surrounding fresh water, under which a gravity flow moves down a slope. The streamline pattern near the head front is shown in Fig. 11(a), and that of the body region in Fig. 11(b). A vigorous mixing between the flow and the fresh water occurs in the body region of the sediment flow. The fresh water motion dies out as shown in Fig. 11(c) where the tail of the flow is displayed.

Figure 12 shows an unsteady streamline pattern near a head similar to the one shown in Fig. 11(a). The unsteady streamline is continuous over the whole flow field in and outside the head. In Fig. 13, the interface

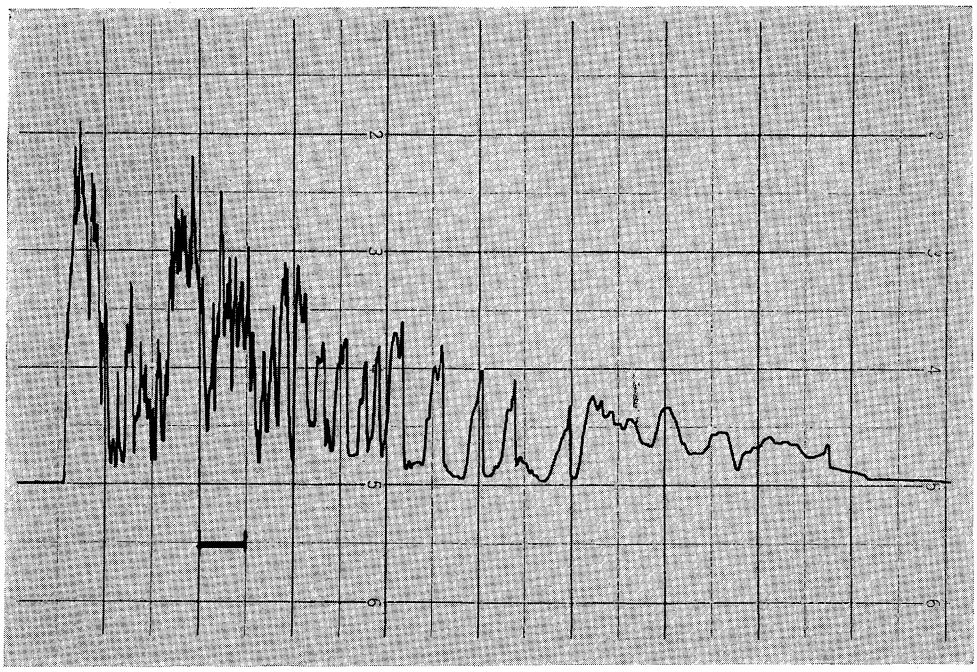

Fig. 10 Velocity fluctuation in a gravity flow of salt solution; $\theta=18°$.

of a head region is shown. The interface shows up the so-called 'secondary ripples'. Figure 14 shows a laminar gravity flow head of a fluid slightly heavier and more viscous than water. The head, visualized with aluminium powder, is almost hemispherical and the body is quite thick.

In Figs. 15(a) to (d), are displayed successive flow patterns of glycerin-water solution visualized by means of the direct shadow method. The flow is fully turbulent, and the outer edges of the neck and body regions are quite irregular. The nose of a head was visualized with a dye line as shown in Fig. 16; the dye line was made by letting a small drop of methylene blue fall slowly through the water before the head has reached there. Figures 17(a) and (b) show the structures of a small quantity of salt solution pushed out of a circular nozzle of 1.5 cm in diameter. These flows were visulized by means of the electrolytic precipitation method. The profile of the flow immediately after its generation is very similar to a head of a type C flow. As time went on, the head was lifted up and became to form a vortex ring. Basically the head of a type C flow may be regarded as a vortex ring moving down a slope. The vortex ring may be laminar or turbulent depending on various parameters related to the sediment.

A series of photographs in Fig. 18 shows the behaviors of a gravity flow of clay in a stratified fluid. The lower layer is a 0.8% salt-solution, and the upper layer is a common water. In Fig. 18(b), the sediment flow is separated from the sloping floor, and moves along the interface between the two fluids. The upper surface of the sediment flow shows a wavy distortion as shown in Figs. 18(b) and (c). As shown in Fig. 18(d), the sediment flow dies out in the course of time. Figures 19(a) to (f) show the intrusion of a clay sediment into an ambient fluid, which is stratified with multiple layers of different densities. In Figs. 19(b) to (d), the flow patterns visualized with aluminium powder indicating interfaces of the stratified fluid would remind of a flow around the leading edge of an aerofoil. Figure 19(e) shows a flow pattern after its front has reached a tank wall, and Fig. 19(f) shows the sediment layer settled down along the interface.

Figures 20(a) to (d) show a gravity flow, which is getting over a semi-circular cylinder placed transversely on the floor of a channel. It will be seen that the fresh water is being taken in behind the cylinder. Figures 21(a) to (d) show the process of passage of a gravity flow about a circular cylinder; the gap between the cylinder and the floor surface is 0.6 cm. Similarly as before, the intake of fresh water occurs behind the cylinder. Figures 22(a) to (d) show a gravity flow down a step with the height of 2.0 cm. The intake of fresh water occurs behind the step. Figure 23 shows a plan view of a gravity flow coming out of a circular nozzle on a sloping floor with $\theta=11°$. The front of the flow is seen to finger out. Figures 24(a) and (b) show the cross sections of a gravity flow falling down vertically from the lower edge of a sloping floor. The instability of this

flow sheet develops downwards as shown in these figures.

We thank Y. Shiraishi and the staff of the marine environment research division of the Res. Inst. Appl. Mech. for their help and interest in this work. A grant from the Ministry of Education, Science and Culture is also acknowledged.

Note added in proof: Recently the motion of the head of a gravity current travelling down a slope was also investigated by Britter & Linden[10], Huppert & Simpson[11], and Honji[12].

Peferences

1) Stanley, D. J. and Swift, D. J. P.: *Marine Sediment Transport and Environmental Management*, John Wiley & Sons, New York, 1976.
2) Allen, J. R. L.: *Physical Process of Sedimentation*, George Allen and Unwin LTD, London, 1977.
3) Komar, P. D.: *Beach Processes and Sedimentation*, Prentice-Hall, Inc., Englewood Cliffs, New Jersey, 1976.
4) Stanley, D. J. and Kelling, G.: *Sedimentation in Submarine Canyons, Fans, and Trenches*, Dowden, Hutchinson and Ross, Inc., 1978.
5) Turner, J. S.: *Buoyancy Effects in Fluids*, Cambridge Univ. Press, 1979.
6) Yih, C-S.: *Stratified Flows*, Academic Press, 1980.
7) Middleton, G. V. and Hampton, M. A.: Subaqueous Sediment Transport and Deposition by Sediment Gravity Flows, in *Marine Sediment Transport and Environmental Management* (Ed. by D. J. Stanley & D. J. Swift), John Wiley & Sons, New York, 1976, Chapt. 11, pp. 197-218.
8) Simpson, J. E.: J. Fluid Mech. **53** (1972) 759.
9) Simpson, J. E. and Britter, R. E.: J. Fluid Mech. **94** (1979) 477.
10) Britter, R. E. and Linden, P. F.: J. Fluid Mech. **99** (1980) 531.
11) Huppert, H. E. and Simpson, J. E.: J. Fluid Mech. **99** (1980) 785.
12) Honji, H.: Flow visualization of underwater avalanches, International Symposium on Flow Visualization, Bochum, Sept. 1980, Preprints, p. 288.

(Received September 26, 1980)

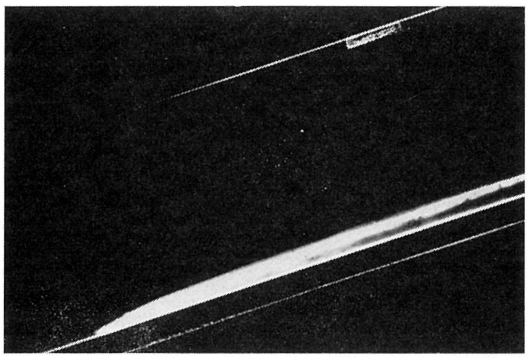

Fig. 3 Type A flow; D=70 μm, θ=18.6°.

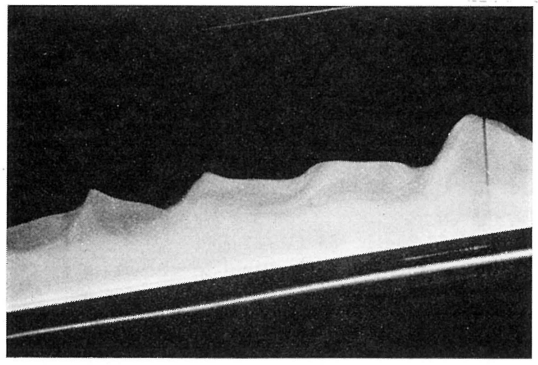

(a) t=0 s.

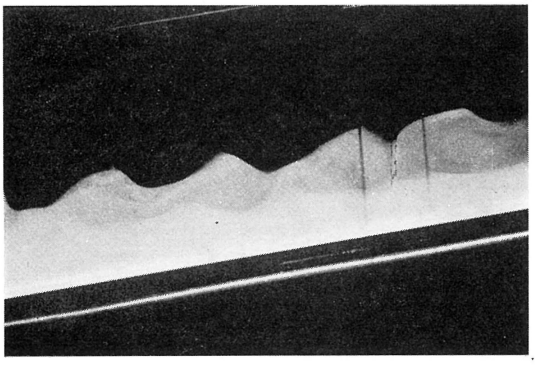

(b) t=30 s.

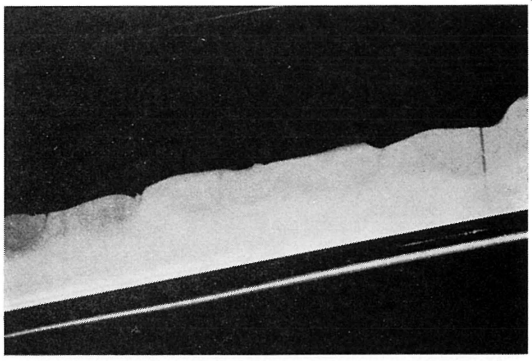

(c) t=50 s.

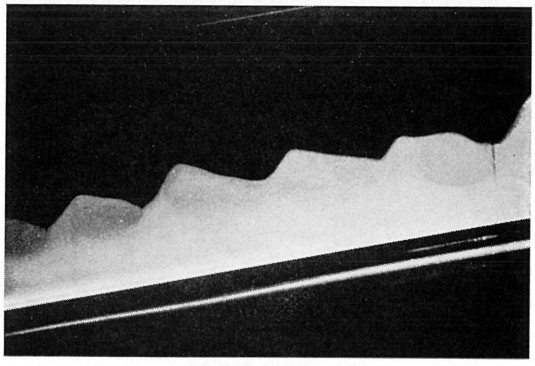

(d) t=70 s.

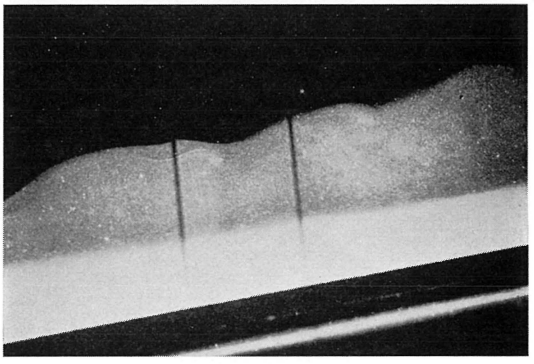

(e) Close-up view.

Fig. 4 Type B flow; D=130 μm, θ=11.5°.

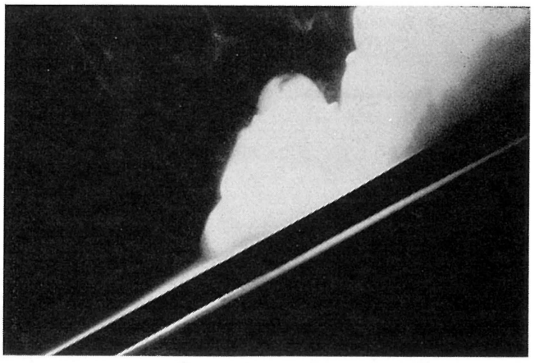

(a) Head region.

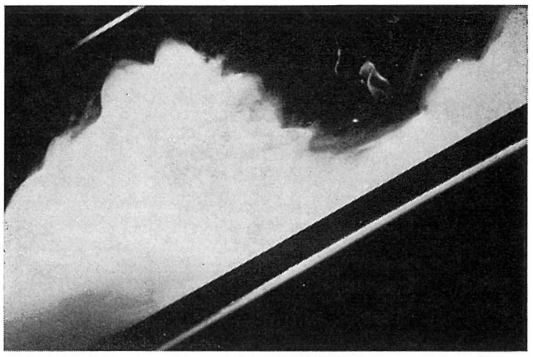

(b) Neck region.

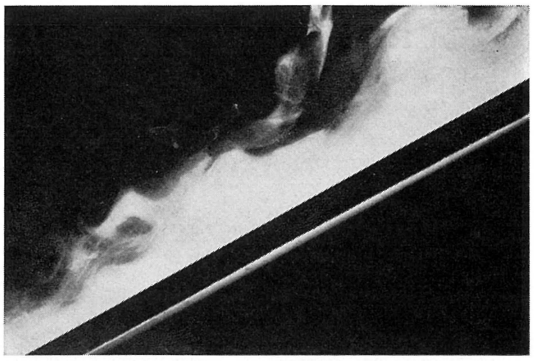

(c) Body region.

Fig. 6 Type C flow; D=6 μm, θ=32°

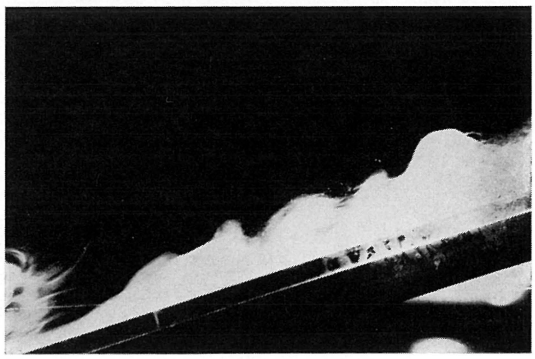

Fig. 8 Lobate structure; D=6 μm, θ=19.5°

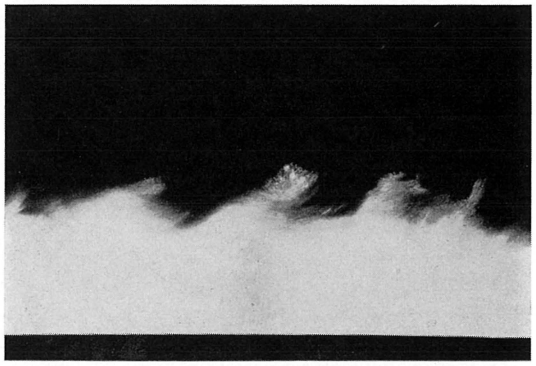

Fig. 9 Developed lobate structure; D=60 μm, θ=30°.

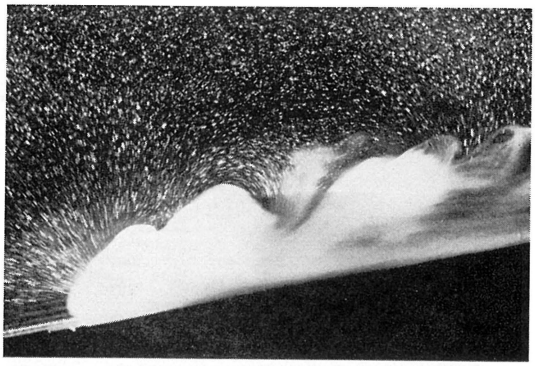

(a)

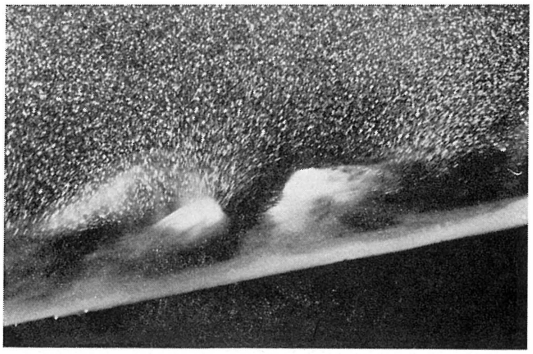

(b)

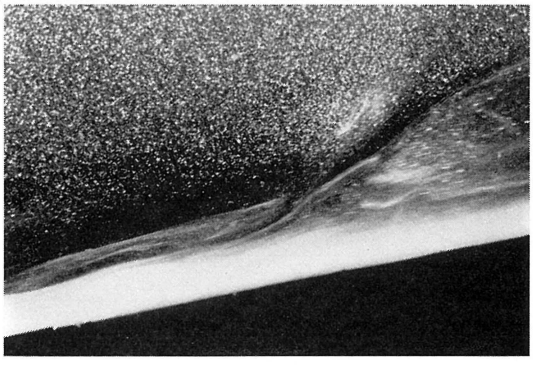

(c)

Fig 11 Unsteady streamline patterns of the motion of a surrounding fresh water; $D=6\,\mu m$, $\theta=11°$.

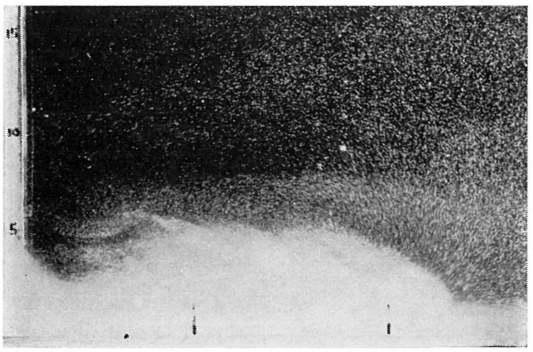

Fig. 12 Close-up view of an unsteady streamline pattern near a head; D=60 μm, θ=0°.

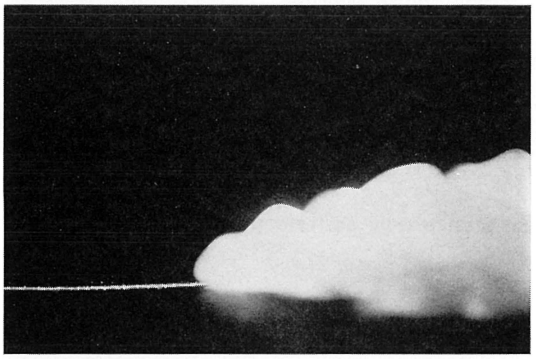

Fig. 13 Secondary ripples on the interface of a head region; D=6 μm, θ=11.3°

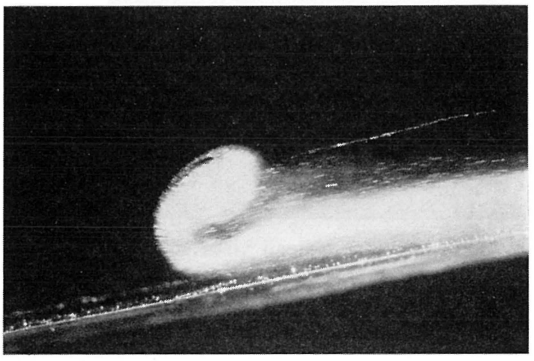

Fig. 14 Laminar gravity flow; θ=11°.

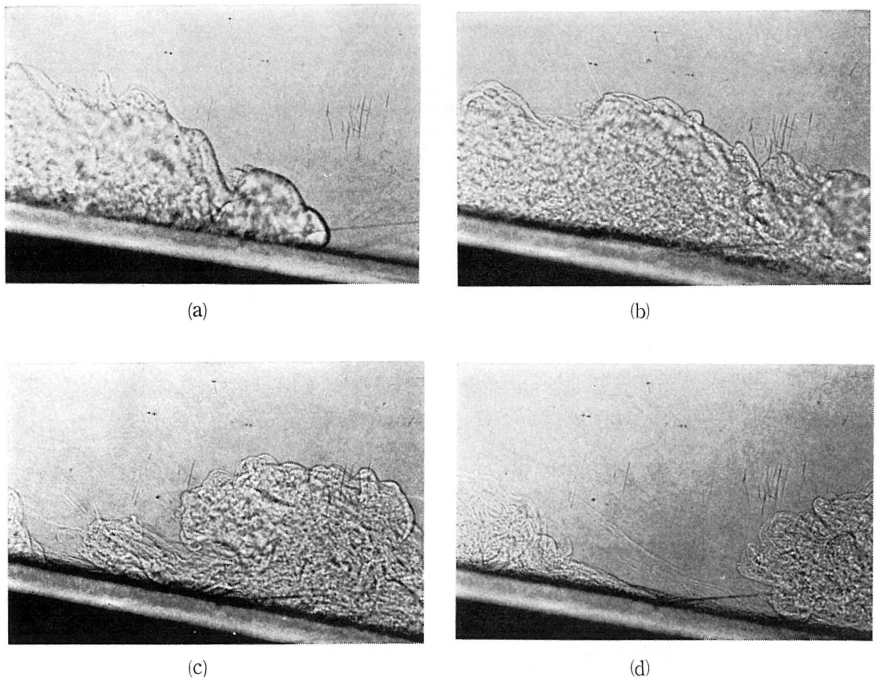

Fig. 15 Successive flow patterns of glycerin-water solution; $\theta=11.5°$.

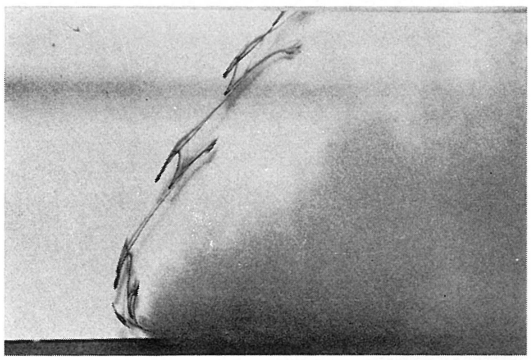

Fig. 16 Front of a head visualized with a dye line;
D=60 μm, $\theta=12.5°$.

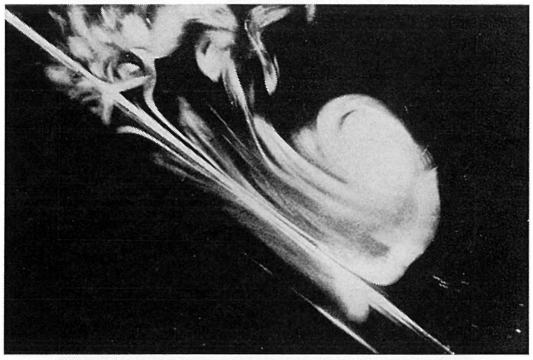

(a)

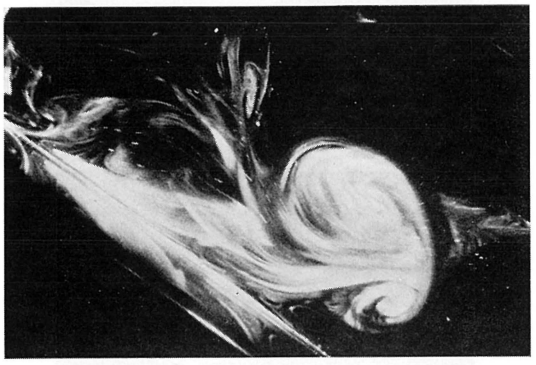

(b)

Fig. 17 Structure of salt solution pushed out of a circular nozzle; $\theta = 36°$.

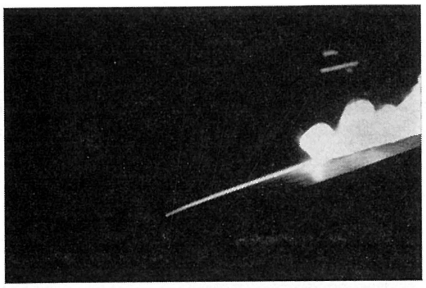

(a)

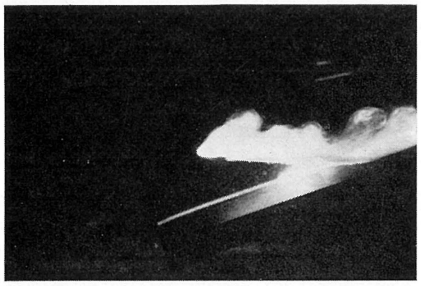

(b)

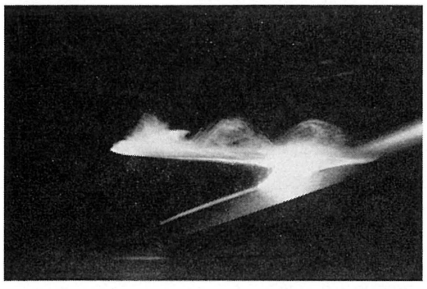

(c)

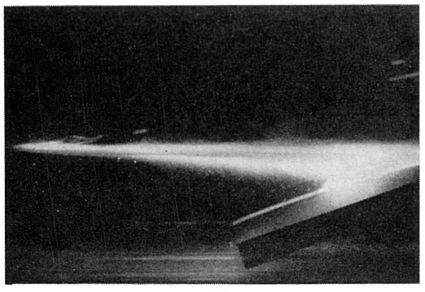

(d)

Fig. 18 Behaviors of a gravity flow of clay in a stratified fluid; D=6 μm, θ=19.5°.

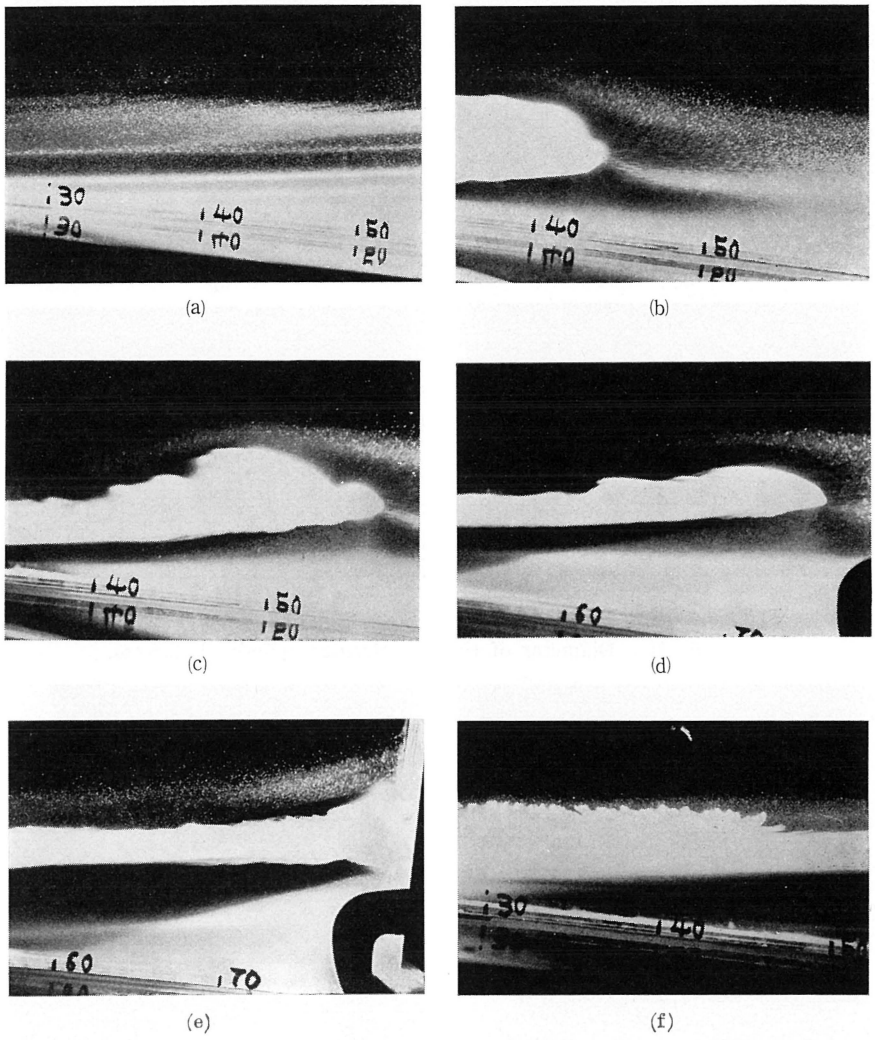

Fig. 19 Intrusion of a clay sediment into the multiply stratified fluid (unit in cm); D=6 μm, θ=7.7°.

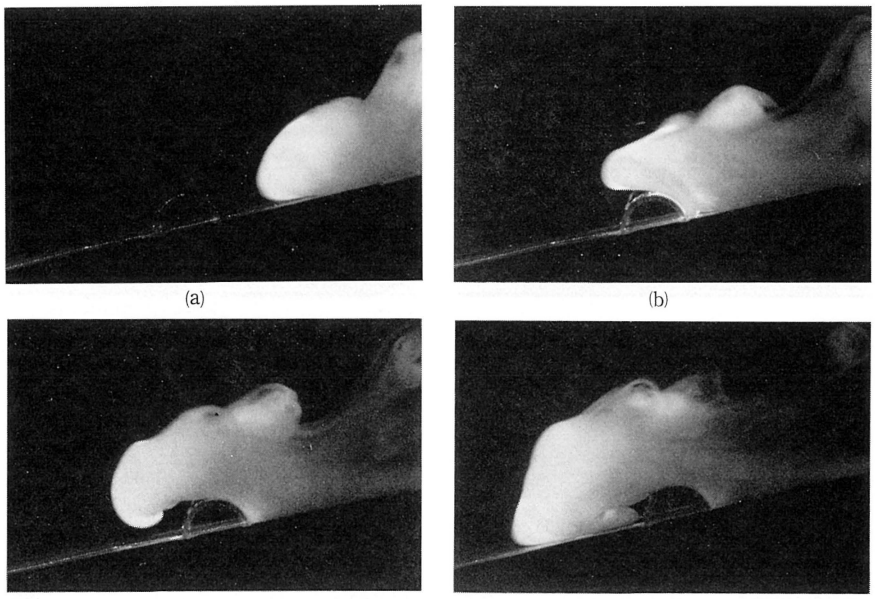

(a) (b)

(c) (d)

Fig. 20 Gravity flow getting over a semicircular cylinder: D=6 μm, θ=11°. Diameter of the semicircular cylinder is 2.5 cm.

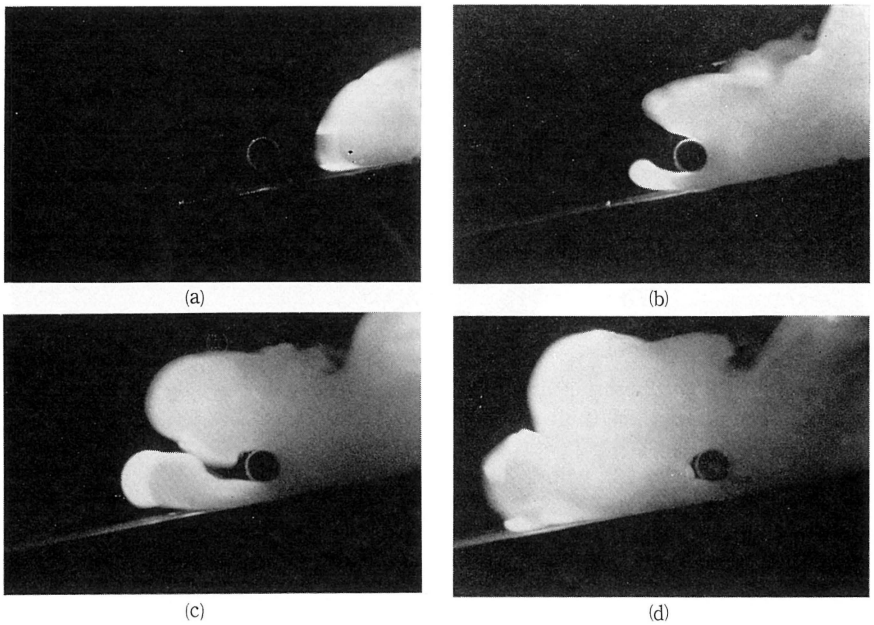

(a) (b)

(c) (d)

Fig. 21 Gravity flow passing over a circular cylinder; D=6 μm, θ=11°. Diameter of the circular cylinder is 1.0 cm and a gap between the cylinder and the floor surface is 0.6 cm.

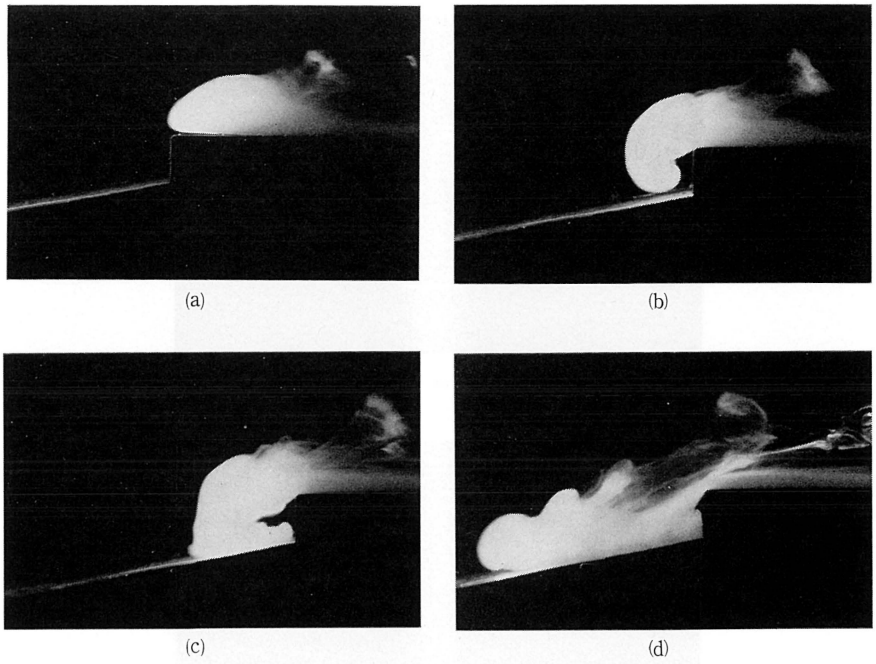

Fig. 22 Gravity flow down a step with the height of 2.0 cm; D=6 μm, θ=11°.

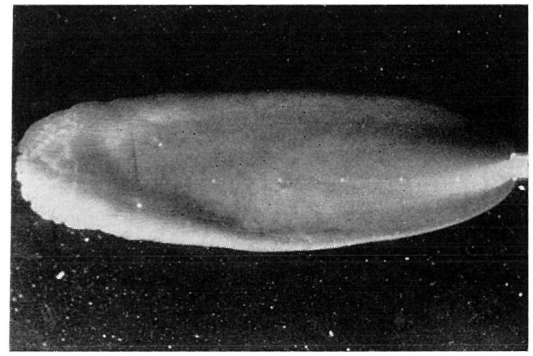

Fig. 23 Plan view of a gravity flow coming out of a circular nozzle on a sioping floor; D=6 μm, θ=11°. Diameter of the nozzle is 1.5 cm.

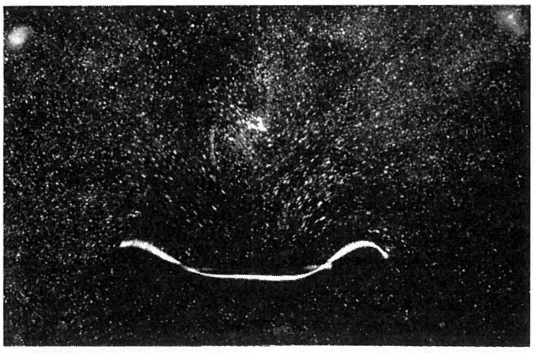

(a)

(b)

Fig. 24 Horizontal cross sections of a gravity flow falling down vertically from the lower edge of a sloping floor; $\theta=20°$. Material is salt solution.